Biomacromol. J., Vol. 5, No. 1, 23-34, July 2019.

Biomacromolecular Journal
www.bmmj.org

Biofunctionalization of Gold Nanorods: A Comparative Study on Conjugation Methods for Fabrication of Nanobiosensors

S. Ranjbari Baglou[a], B. Ranjbar[a,b,*] and T. Tohidi Moghadam[a]

[a]*Department of Nanobiotechnology, Faculty of Biological Sciences, Tarbiat Modares University, Tehran, Iran*

[b]*Department of Biophysics, Faculty of Biological Sciences, Tarbiat Modares University, Tehran, Iran*

(Received 29 July 2019, Accepted 25 September 2019)

ABSTRACT

Gold Nanorods have promised variety of applications in biomedicine and biosensing. As a fruitful candidate for early detection and imaging, these plasmonic nanoparticles have been utilized for diagnostic applications of interest. However, prior to design and fabricate SPR-based nanobiosensors, the type and nature of conjugation with biomolecules would be of utmost importance. Herein, four strategies have been used for biofunctionalization of gold nanorods with a specific oligonucleotide sequence, *i.e.* "Direct", "Salt-aging", "Rapid Modification at Low pH" and "Anionic Surfactant Mediated" methods. The nanoprobe, biofunctionalization process and probability of unspecific aggregations after purification have been investigated by monitoring the characteristic transverse and longitudinal surface plasmon resonance bands of the nanostructure. Formation of the GNR-DNA nanobioconjugate was traced by FTIR spectroscopy. Comparison of the four conjugation methods showed that using anionic surfactant (SDS) would be useful in efficient biofunctionalization of GNRs, without perturbation of its rod morphology. Results of this effort could pave the way for design and fabrication of SPR based nanobiosensors in the upcoming optical diagnostic strategies.

Keywords: Gold nanorods, Surface plasmon resonance, Biofunctionalization, Nanoprobe

INTRODUCTION

With recent advances in nanobiotechnology, researchers have developed new techniques in molecular diagnosis and early detection strategies. Amongst various tiny nanostructures, plasmonic nanoparticles have been nominated as good candidates for biomolecular detection purposes, giving quick response to trace changes in the refractive index and local environment.

In the light of nanobiosensing and early diagnosis, gold nanorods with unique optical properties and sensitive surface plasmon resonance (SPR) characteristics offer promising capability for monitoring the existence of a biomolecule of interest. In general, SPR phenomenon results from the incident electromagnetic radiation and interactions with electron of conducting layer in plasmonic metals, which ultimately leads to collective oscillation of electrons in a specific wavelength [1,2]. This feature of plasmonic nanoparticles is responsible for their distinctive color and outstanding properties [3]. So far, variety of applications have been proposed for gold nanorods, *i.e.* in genomics [4], detection and biosensors [5], immunoanalysis, clinical chemistry, photothermolysis of microorganisms and cancerous cells, targeted gene and drug delivery [6], optical bioimaging and study of damaged tissues [7], programmable origami of advanced structures [8,9], *etc*. To fulfill such goals, gold nanorods (GNRs) are often functionalized with biomolecules of interest, such as antibodies, aptamers, specific sequences of single/double stranded oligonucleotide, *etc.* Particularly, when strands of oligonucleotides are designed for conjugation with GNR matrix, some challenges in the functionalization process come into the picture [4,10-13]. At times, loss of rod morphology and non-specific aggregation of the nanostructures is inevitable. Targeted interaction of sequences with GNRs through covalent bond is a routine strategy that is accomplished by several methods. The simplest one is direct method in which, the functional

*Corresponding author. E-mail: ranjbarb@modares.ac.ir

sequence is mixed up with nanorods without addition of any other agents [4]. This method requires several days for conjugating the sequence with GNR matrix. In another strategy named "round-trip phase transfer", thiolated sequences attach to GNR surface by ligand exchange of the nanostructure and provide the surface linkage via disulfide bonds [12]. "Gradual salt-aging" is the other technique, which enhances the quantity of oligonucleotide loading and stability of the functionalizing environment [13]. Further methods such as "in situ hybridization" [10] and "rapid modification at low pH (RMLP)" [11] have been also reported. In the first, cationic surfactant of Cetyl trimethylammonium bromide (CTAB) is replaced by carboxylated surfactant for the purpose of amide bond formation (between carboxylated GNRs and amine fuctionalized sequence). The latter enables extremely large amounts of oligonucleotide conjugation.

Depending on the type of application and the sensitive nature of GNRs (due to the aggregation tendency of particles at nanoscale), it is not advised to generalize a single, particular method for bioconjugation. For example, in a conjugation process including thiolation of the nanostructure matrix, the weak and complicated bond between sulfur groups and the surrounding silver (contributed in elongation of nanorods) interferes in formation of Au-S bond [14,15]. Furthermore, gold nanorods are typically synthesized in the presence of excess cationic surfactant (CTAB), both as a chemical stabilizer and director of rod morphology. Perturbations in the bilayer of this surfactant or excess purification would induce irreversible aggregation [14,16]. Therefore, prior to design and fabricate any type of nanobiosensor with such rod shaped nanostructures, finding a proper bioconjugation strategy would be of utmost importance. This report is a fundamental study on a couple of bioconjugation techniques, including "direct", "salt-aging", "rapid modification at low pH" and "anionic surfactant mediated" methods, to find the most favorable strategy, leading to a stable, functionalized GNR-DNA complex, *i.e.* nanoprobe. The nanoprobe is mainly monitored by changes in the characteristic surface plasmon resonance (SPR) bands of GNRs, and the functionalization was confirmed by Fourier transform infrared (FTIR) spectroscopy.

MATERIALS AND METHODS

Materials

All materials, except some cases, were purchased from Sigma. Sodium chloride and ethyl acetate solution were prepared by Dr. Mojallali Chemical Labs. Tris-base, boric acid, and ethylenediaminetetraacetic acid (EDTA) were provided from Merck, Romil, and Cinaclone, respectively. Thiolated sequence of (SH)-(CH2)6-5′-ACAGGCCGGGA-3′ was procured from Faza Biotech Co. In all experiments, sterile distilled water was used. Glassware was carefully cleansed with a dilute solution of sulfonic acid and rinsed with deionized water.

Methods

Synthesis of gold nanorods. Gold nanorods were synthesized *via* sequential seed mediated growth method [17,18]. Briefly, small spherical gold nanoparticles of size below 5 nm (seeds) were prepared by mixing 250 µl of 0.01 M $HAuCl_4 \cdot 3H_2O$ aqueous solution with 7.5 ml of 0.095 M surfactant (CTAB). The reduction reaction started by immediate addition of 600 µl 0.01 M ice-cold $NaBH_4$ solution to the medium. The reactants were mixed by rapid inversion for two minutes and kept undisturbed at room temperature. It will take a minimum of 2 h for seed particles to grow in the solution. For the growth step, 9.5 ml of 0.095 M CTAB, 400 µl of 0.01 M $HAuCl_4 \cdot 3H_2O$, 60 µl of 0.01 M $AgNO_3$ and 64 µl 0.10 M ascorbic acid solutions were mixed mildly. Finally, 40 µl of seed particles was added, shaken gently for 10 s. The reaction mixture was kept undisturbed for at least 3 h.

Purification and characterization of gold nanorods. To remove excess cationic surfactant and unreacted gold ions, gold nanorods were purified by two rounds of centrifugation (14,000 rpm for 7 min). After decanting the supernatant, samples were diluted with ddH_2O. To disperse the particles in the solution, samples were resuspended in ultrasonicator water bath for 15 min. To confirm the rod morphology of the nanostructures, samples were characterized by UV-Vis absorption spectrophotometer, Carry-100 (400-900 nm). To characterize the shape and size of samples, gold nanorods were deposited on a carbon coated copper grid. Samples were kept undisturbed and

dried for 30 min, and characterized on a Ziess EM10C transmission electron microscopy.

Preparation and Reduction of Thiolated Sequence

To reduce sulfur group of the sequence, a protocol provided by Bioneer was followed with some modifications. Thiolated sequence (50 µl, 1 µM in HEPES 25 mM) was treated with 60 mM of the reducing agent dithiothreitol (DTT), and kept for one hour. To remove untreated and excess DTT, an equivalent volume of the probe solution and ethyl acetate were mixed and vortexed. The solution was kept undisturbed to reach a biphasic environment. The upper phase containing organic solvent and DTT was decanted to leave the lower aqueous phase with reduced thiol groups. The extraction process was repeated three times. The ready reduced sequence was immediately mixed with GNRs. The following methods were used for GNR-DNA nanobioconjugates (nanoprobes).

Direct method. This method was reported by Chen and colleagues [4]. Purified GNRs (1 OD) were mixed with different concentrations of the oligonucleotide. For proper conjugation, the mixture was incubated at ambient temperature for several days. To remove the unbound sequence, the nanoprobe was centrifuged, and the pellet was redispersed in preservative buffer, containing 10 mM HEPES, 0.01% SDS and 100 mM NaCl.

Salt-aging method. Firstly, the oligonucleotide sequence was mixed with nanoparticles [13]. Secondly, anionic surfactant of SDS was added to a final concentration of 0.01%. The sample was ultrasonicated for 20 s and left undisturbed from 2-24 h at room temperature. To increase DNA loading, NaCl (1 M) was gradually added to the medium, to the final concentration of 100 mM with 2 h intervals. The nanoprobe was purified the next day, and the pellets were redispersed in preservative buffer.

Rapid modification at low pH (RMLP) method. In this method, thiolated sequences were used both in the reduced and non-reduced forms [11]. The initial buffer included 0.02% SDS, 1xTBE (Tris-base/boric acid/EDTA) and 500 mM NaCl (pH = 3). Thiolated DNA and GNRs were added to the buffer solution, giving a final GNR of 1 OD. The mixture was gently shaken for 10 min, centrifuged repetitively and re-suspended in buffer, containing 1xTBE and 100 mM NaCl, with three different pH values (3, 5 and 7).

Anionic surfactant mediated method. The reduced thiolated sequences were added to GNRs slowly. Anionic surfactant (1% SDS) was added dropwise to achieve final concentration of 0.01%. The solution was then ultrasonicated in water bath for 10 s at ambient temperature. The mixture was further kept for 24 h. The nanoprobe was centrifuged and redispersed in buffer, containing HEPES 10 mM and 0.01% SDS. Finally, 10 mM of NaCl was added to the samples.

Fourier Transform Infrared Spectroscopy (FTIR)

To monitor linkage of the thiol group to GNR matrix, samples were characterized by FT-IR spectroscopy. The nanoprobe was lyophilized, and the homogeneous powder was mixed with potassium bromide. PerkinElmer-Frontier model was used in the range of 400-4000 cm^{-1}.

RESULTS AND DISCUSSION

The first technique to evaluate formation of nanostructures with rod morphology is studying plasmonic absorption profile of the particles (Fig. 1). As shown in the figure, two characteristic surface plasmon resonance bands appeared in the visible and near infrared region, typically known as transverse (TSPR) and longitudinal (LSPR) bands for GNRs. The second peak of higher intensity is attributed to collective oscillation of conduction band electrons on the length of the nanostructures. High intensity and sensitivity of this SPR band to trace changes in the local environment, along with high absorption cross sections, nominates GNRs as fruitful candidates in theranostic approaches. The inset (Fig. 1) depicts transmission electron microscopy image of GNRs, confirming formation of nanostructures with rod morphology. Accordingly, the average aspect ratio of GNRs was estimated to be 3.12, with average length of 34 nm.

Figure 2 shows changes in the SPR bands of GNR-DNA complex (nanoprobe) with different concentrations of the oligonucleotide, prepared by direct method. After performing purification process, the characteristic LSPR peak of pristine GNRs (without thiol modification) appeared at 710 nm, which decreased notably upon addition of oligonucleotide sequence. A glance at Fig. 2 shows that the nanostructure has lost its particular rod morphology upon

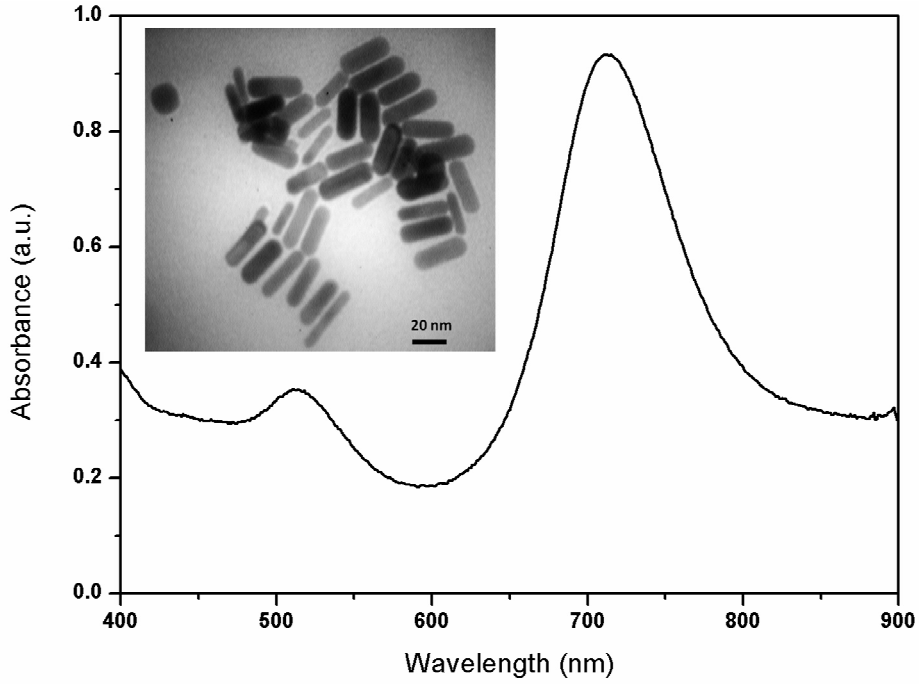

Fig. 1. Characteristic SPR bands and TEM image (the inset) of GNRs.

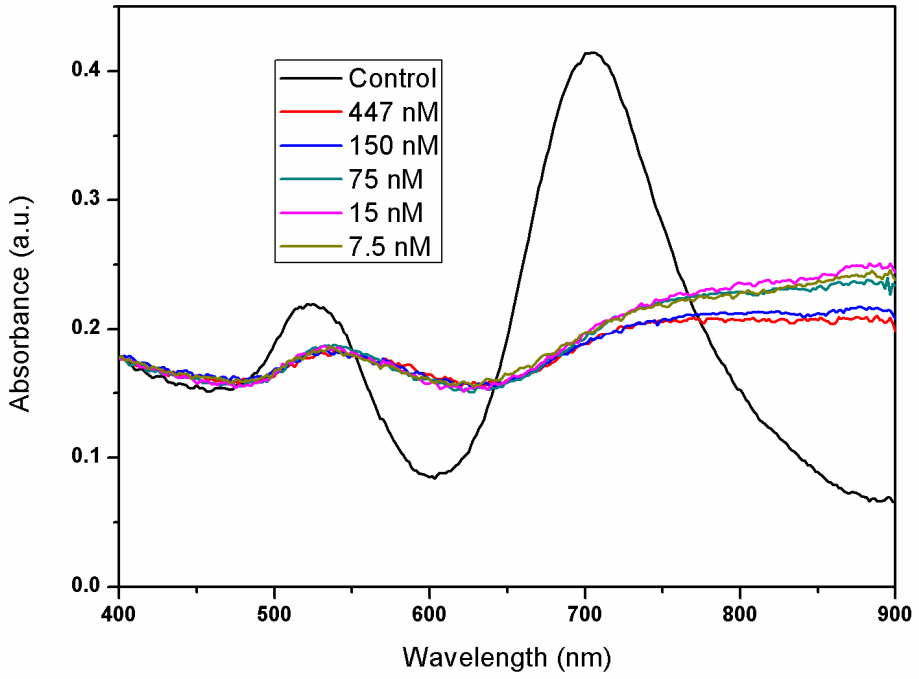

Fig. 2. SPR bands of Nanoprobe with different concentrations of DNA, prepared by direct method.

interaction with biomolecule, leading to disappearance of both TSPR and LSPR bands. This phenomenon reflects notable decrease in interparticle decrease and aggregation of the nanostructures. As mentioned earlier, gold nanorods are synthesized in a medium containing excess cationic surfactant (CTAB), which plays critical role in dictating the rod morphology for the nanostructures. Presence of amine groups in the surfactant structure provides positive charge onto the matrix of GNRs [19,20]. Meanwhile, addition of single-stranded DNA to nanorods, makes a ternary complex of ssDNA-CTAB-GNR, giving rise to electrostatic interactions between the polyanionic phosphate chain in oligonucleotides and the cationic surfactant bilayer of CTAB around nanorods [20,21]. Such type of interaction might be responsible for aggregation of GNRs upon direct addition of oligonucleotides. It is also worth to mention that presence of three adenine nucleotides and lack of thymine group in the oligonucleotide sequence might make it more prone to physical adsorption [8,22]. Therefore, direct method does not seem very efficient for adenine-rich and poor/lacking thymine sequences.

Figure 3 depicts the effect of NaCl addition on absorption profile of the nanoprobe with different oligonucleotide concentrations. In the presence of salt ions in nanoprobe's environment, increasing oligonucleotide concentration from 10 to 100 nM resulted in decrease of both transverse and longitudinal surface plasmon resonance bands. Before performing the purification process, the nanoprobe shows stability, maintaining its rod morphology up to 30 nM of oligonucleotide concentration (Fig. 3a). Meanwhile, a glance at Fig. 3b shows that centrifugation notably decreased the nanoprobe stability, dictating severe decrease in interparticle distance and aggregation of the nanostructures. It is noteworthy that the nanoprobe with minimum oligonucleotide concentration (10 nM) has remained unperturbed even after the purification process (Fig. 3b).

In the next step, the optimal concentration of salt was studied by frequent addition of NaCl. With two times of salt addition (up to 50 nM), it was noticed that the nanoprobe is quite stable before centrifugation (Fig. 4a); whereas it finds tendency for aggregation after purification process (Fig. 4b). Only samples without salt treatment were unperturbed in this experiment. It could be assumed that ionic strength plays a dual role in the biofunctionalization process of gold nanorods. On the one hand, interaction of DNA and GNRs is partially controlled upon increment of ionic strength [23], and on the other hand, ionic strength of the complex environment plays a critical role as a contributing factor in aggregation phenomenon [8].

The third method for biofunctionalization was performed at low pH, based on Shi's *et al.* report [17]. Since disulfide bonds are converted to protonated thiol groups in the acidic environment [32], functionalization of GNRs has been studied under both reducing and non-reducing conditions (Fig. 5). The acidic environment (pH 3) is a strong proton donor, thereby reducing the sulfide group [32]. Monitoring SPR bands of the nanoprobe reflected its stability in case of using non-reduced sequences (Fig. 5). While DTT is a strong reductive agent at pH 5, it is not sufficiently strong at lower pH values. It is also noteworthy to mention that extracting excess DDT by ethyl acetate, rather than using NAP-5 columns, might cause inefficient DDT removal, thereby affecting the conjugation process and stability of the nanoprobe.

Furthermore, the nanoprobe was homogenized at three different pH values 3, 5 and 7 (pH value has not been mentioned in Shi's *et al.* report). Changes in SPR bands were compared with control (Fig. 5b). While there wasn't any remarkable difference for all three pH values, intensity of LSPR band decreased notably with respect to the control sample. Moreover, a broad, low intensity band appeared in longer region of the wavelength, which might have raised due to end-to-end assembly and local aggregation of GNRs [24,25]. It is also worth to mention that in other reports, either the LSPR intensity of the nanoprobe has not been shown [11], or represented with much more decrease in its absorption intensity [26]. Considering the interaction mechanism, adenine and cytosine nucleotides gain positive charge in acidic environment. Although SDS is present in the medium, a set of three cytosines, and three adenines contribute a high proportion of 11-mer sequences. Hence, presence of positively charged nucleotides in the acidic solution induces electrostatic repulsions between CTAB coated GNRs and oligonucleotide sequence, decreasing the chance of linking for thiol group and formation of Au-S bonds [8,11].

Based on the above strategies and absorption profiles of

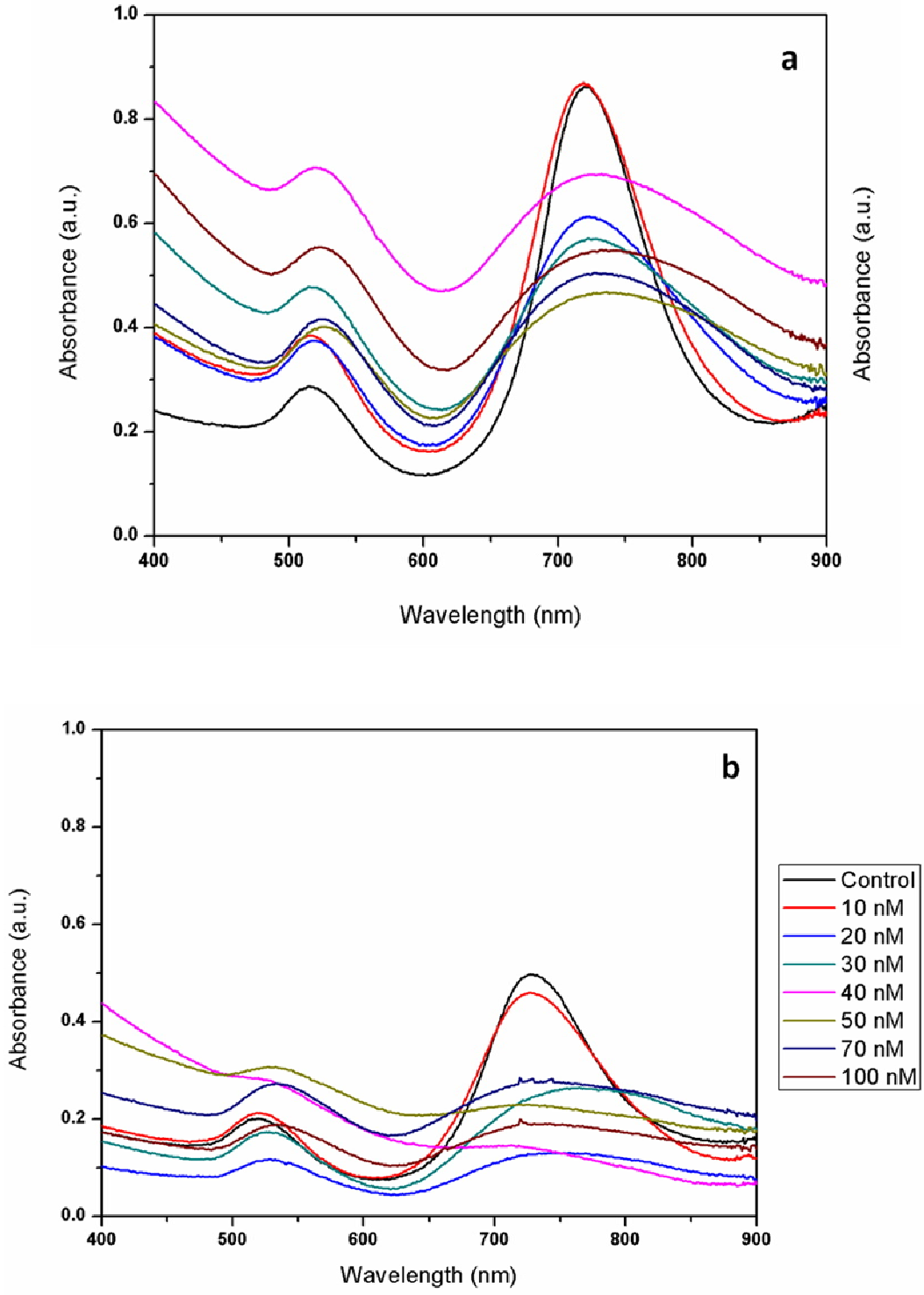

Fig. 3. SPR bands of nanoprobes with different concentrations of DNA, prepared by salt-aging method, (a) before and (b) after centrifugation.

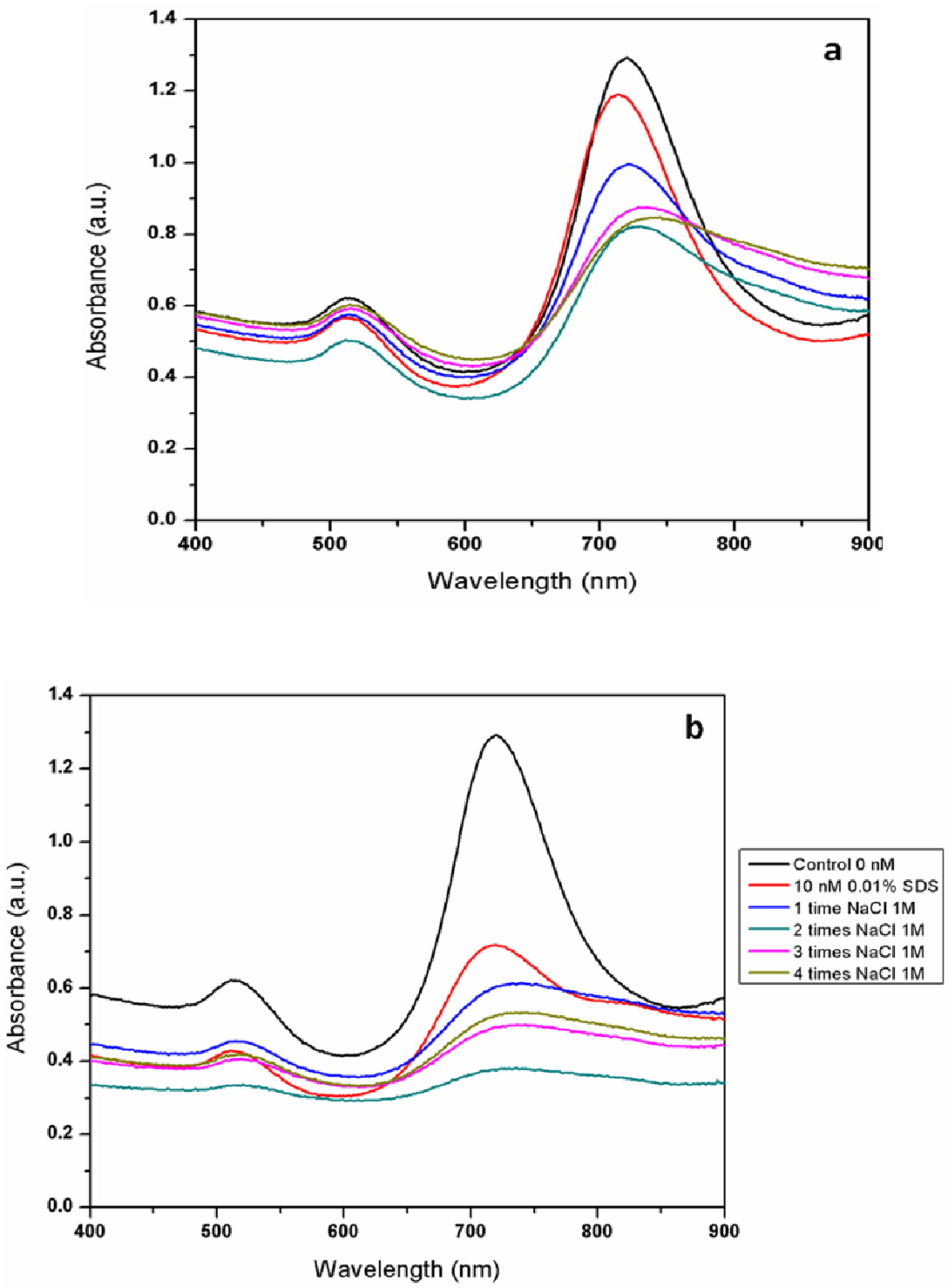

Fig. 4. SPR bands of nanoprobes prepared by salt aging method. The nanoprobe was treated with NaCl (1-4 times) 25, 50, 75 and 100 mM (a) before and (b) after centrifugation.

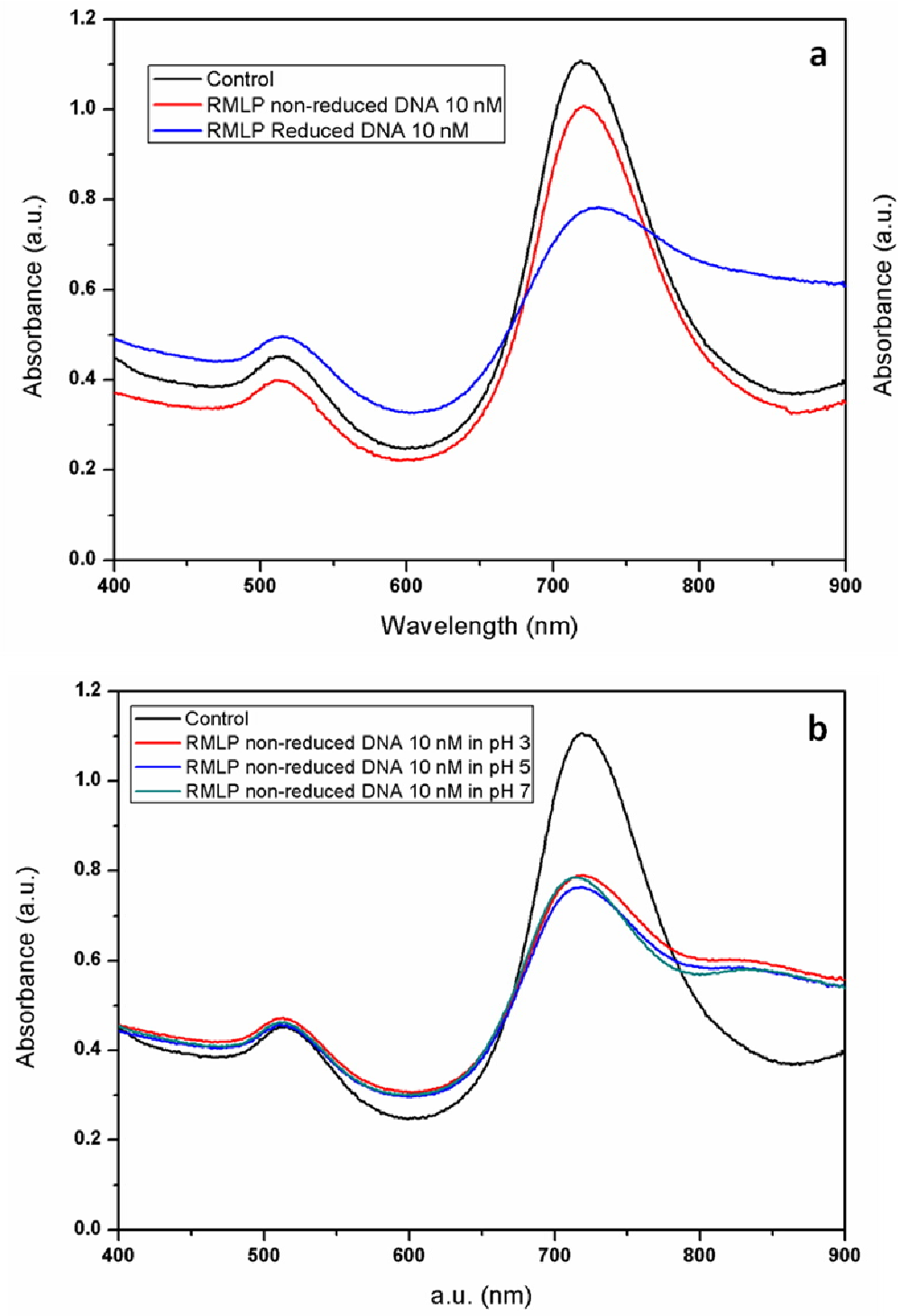

Fig. 5. SPR bands of nanoprobes prepared by RMLP method, (a) with reduced and non-reduced thiolated DNA before centrifugation, and (b) non-reduced DNA after centrifugation (pH 3, 5 and 7).

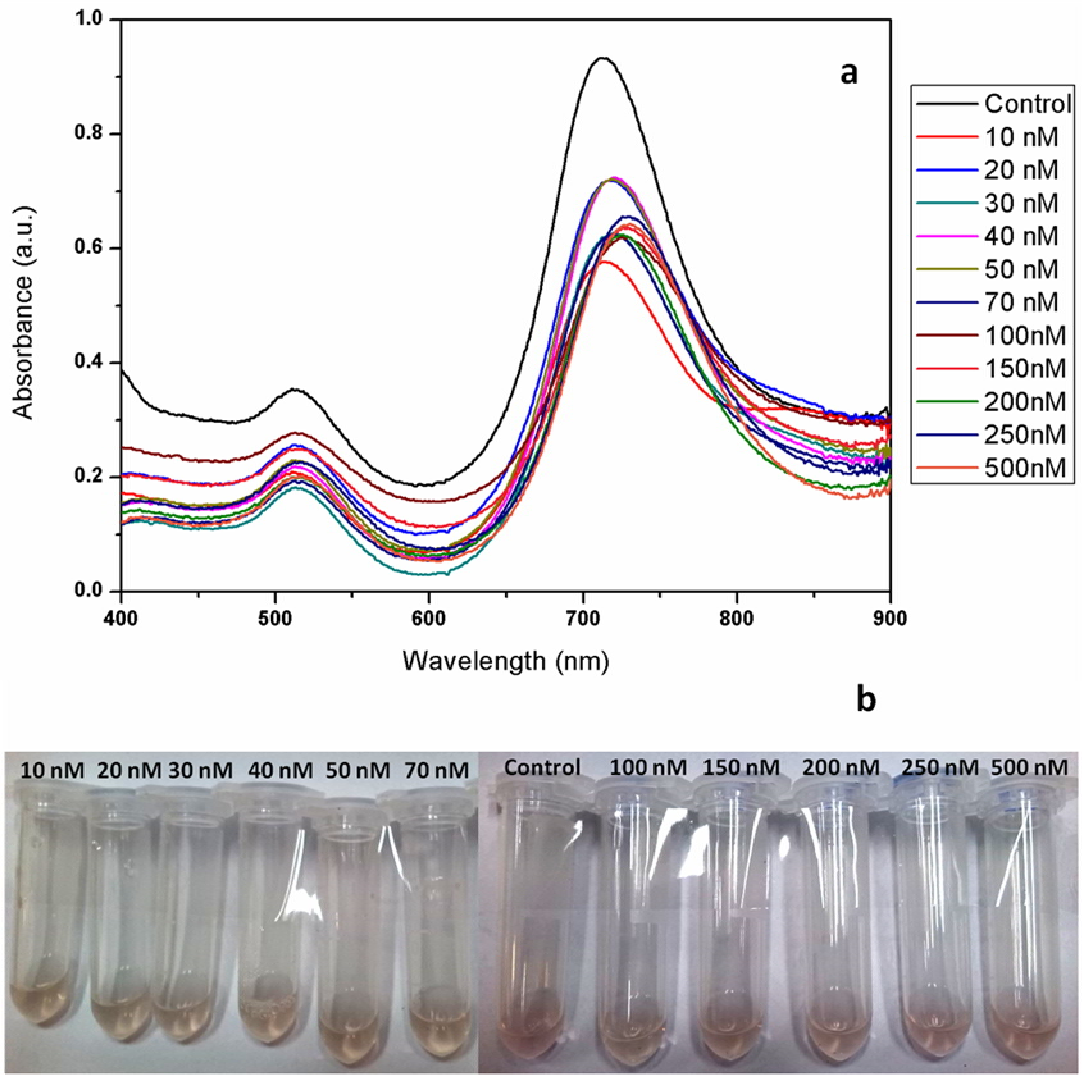

Fig. 6. (a) SPR bands of nanoprobes with different concentrations of oligonucleotides, in SDS, and (b) Appearance of nanoprobes after centrifugation.

the nanoprobes, the effect of anionic surfactant (SDS) was also studied on the biofunctionalization process. Figure 6 depicts SPR bands and appearance of nanoprobe samples (with different concentrations of oligonucleotide sequences) in the presence of anionic surfactant. As shown in Fig. 6a, the nanoprobes remain highly stable upto a final concentration of 250 nM DNA, even after centrifugation. Although intensity of LSPR band has notably decreased at 500 nM (oligonucleotide), is has perfectly maintained the rod morphology, without considerable change in interparticle distance (see Fig. 6a). In addition, appearance of nanoprobe is clear and uniform (Fig. 6b). Therefore, the anionic surfactant did not induce any morphological perturbations in the nanoprobe.

Therefore, surfactant mediated conjugation technique is considered to be useful, due to replacement of cationic long-chain CTAB with short-chain anionic SDS around GNRs. Probably, SDS reduces electrostatic interaction of oligonucleotide sequences with nanostructures, meanwhile stabilizing them [27]. On the other hand, the anionic

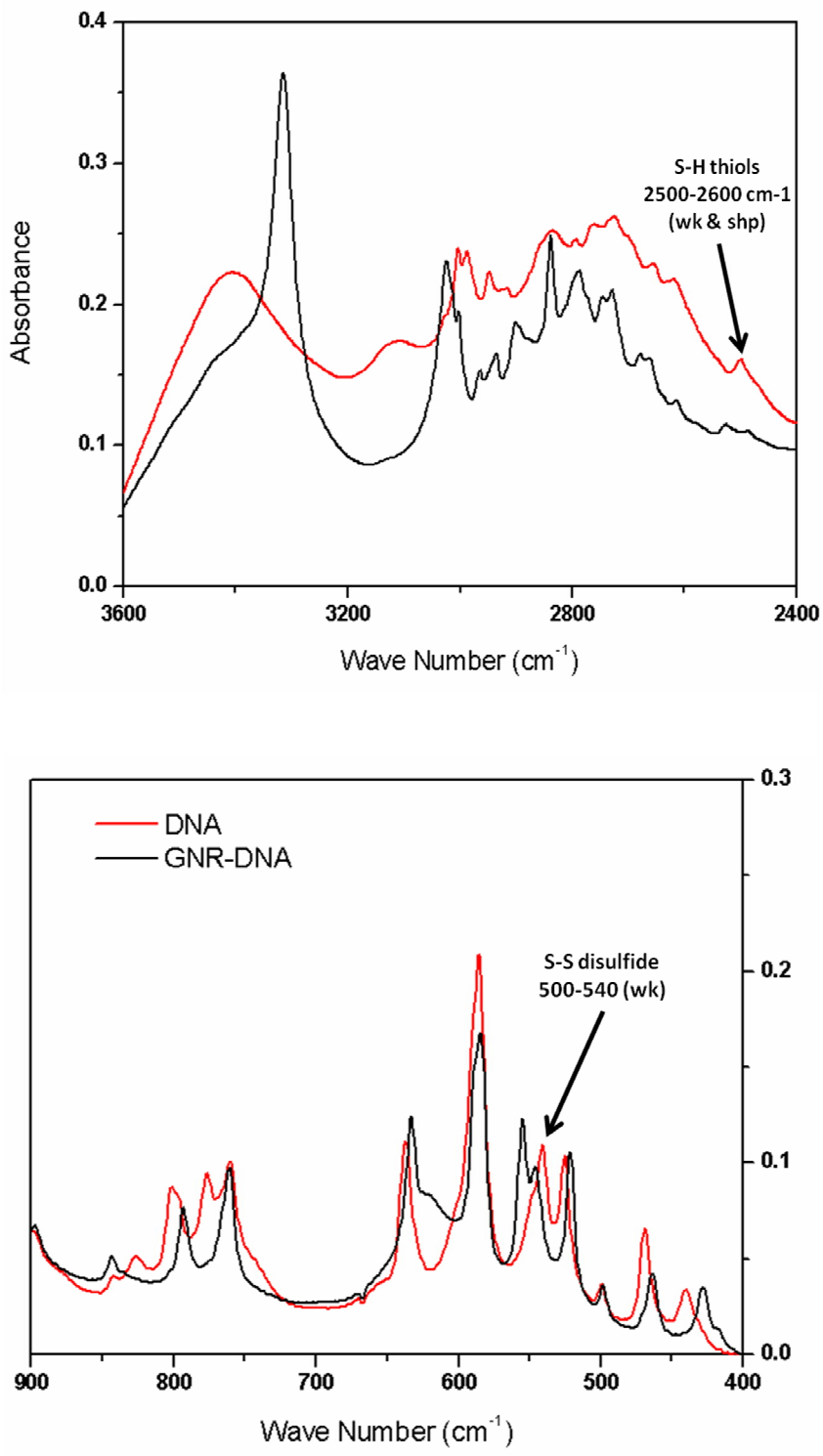

Fig. 7. FTIR spectra of thiolated DNA before and after conjugation with GNRs.

surfactant unfolds the tertiary structure of oligonucleotide and facilitates availability of the thiol groups [27]. As the final step, keeping the purified nanoprobes in 10 mM NaCl solution would increase the ionic strength and stabilize the nanoprobe [23,28].

In order to confirm formation of Au-S bonds, FTIR was used (Fig. 7). A weak but apparent peak around 2500 cm^{-1} represents free thiol group in the oligonucleotide sequences (S-H). Upon formation of GNR-DNA complex, the band has been vanished, clearly showing formation of Au-S bond [29,30]. In the long region of the wavelength, thiolated sequence shows a poor peak at 540 cm^{-1}, indicating trans-gauche-trans conformation of some disulfide bridges [31]. However, the peak of disulfide bond is of low intensity for the nanoprobe.

To summarize, comparison of the four conjugation methods discussed above, showed that using anionic surfactant (SDS) would be useful in efficient biofunctionalization of GNRs, without perturbation of its rod morphology.

CONCLUSIONS

Gold nanorods (GNRs) have been nominated as prosperous candidates in theranostic applications. To fulfill the goal of using these tiny nanostructures in designing new generation of nanobiosensors, it is important to conduct a series of fundamental studies on biofunctionalization processes, their efficiency and probable interference in interparticle distance and perturbation of morphology. This report has focused on a comparative study, investigating four strategies for conjugation of GNRs and Oligonucleotide as biomolecule of interest. Direct, salt-aging, rapid modification in acidic condition, and anionic surfactant mediated conjugation strategies showed utility of anionic surface active agent (the last method) as the most appropriate choice for biofunctionalization of GNRs. The nanoprobe retained its stability over time, even after the purification process. Results of this effort could pave the way for design and fabrication of SPR based nanobiosensors in the upcoming optical diagnostic strategies.

ACKNOWLEDGMENTS

The authors would like to acknowledge financial support provided by Tarbiat Modares University, and express their sincere gratitude to Negar Nadafi, Dr. Zahra Rezaei, Amir Zaheri and Dr. Saeed Pourjafari.

REFERENCES

[1] P.N. Sisco, "Gold Nanorods: Applications in Chemical Sensing, Biological Imaging and Effects on 3-Dimensional Tissue Culture," University of Illinois at Urbana-Champaign, 2011.

[2] J. Stone, S. Jackson, D. Wright, Rev. Nanomedicine Nanobiotechnology 3 (2011) 100.

[3] K.E. Roskov, K.A. Kozek, W.-C. Wu, R.K. Chhetri, A.L. Oldenburg, R.J. Spontak, J.B. Tracy, Langmuir 27 (2011) 13965.

[4] C.-C. Chen, Y.-P. Lin, C.-W. Wang, H.-C. Tzeng, C.-H. Wu, Y.-C. Chen, C.-P. Chen, L.-C. Chen, Y.-C. Wu, J. Am. Chem. Soc. 128 (2006) 3709.

[5] Y. Zhu, D. Qiu, G. Yang, M. Wang, Q. Zhang, P. Wang, H. Ming, D. Zhang, Y. Yu, G. Zou, R. Badugu, J.R. Lakowicz, Biosens. Bioelectron. 85 (2016) 198.

[6] X. Huang, P.K. Jain, I.H. El-Sayed, M.A. El-Sayed, Photochem. Photobiol. 82 (2006) 412.

[7] A.V. Liopo, A. Conjusteau, O.VChumakova, S.A. Ermilov, R. Su, A.A. Oraevsky, Nanosci. Nanotechnol. Lett. 4 (2012) 681.

[8] Q. Liu, C. Song, Z. Wang, N. Li, B. Ding, Methods, 67 (2014) 205.

[9] Q. Jiang, Y. Shi, Q. Zhang, N. Li, P. Zhan, L. Song, L. Dai, J. Tian, Y. Du, Z. Cheng, B. Ding, Small. 11 (2015) 5134.

[10] H. Chen, F. Xu, S. Hong, L. Wang, Spectrochim. Acta- Part A Mol. Biomol. Spectrosc. 65 (2006) 428.

[11] D. Shi, C. Song, Q. Jiang, Z.-G. Wang, and B. Ding, Chem. Commun. 49 (2013) 2533.

[12] A. Wijaya, S.B. Schaffer, I.G. Pallares, K. Hamad-Schifferli, ACS Nano 3 (2009) 80.

[13] H.J. Parab, C. Jung, J.H. Lee, H. Gyu, H.G. Park, Biosens. Bioelectron. 26 (2010) 667.

[14] Y. Wang, D. Aili, R. Selegard, Y. Tay, L. Baltzer, H. Zhang, B. Liedberg, J. Mater. Chem. 22 (2012) 20368.

[15] M.R. Jones, R.J. Macfarlane, B. Lee, J. Zhang, K.L. Young, A.J. Senesi, C.A. Mirkin, Nat. Mater. 9 (2010) 913.

[16] L. Vigderman, B.P. Khanal, E.R. Zubarev, Adv. Mater. 24 (2012) 4811.

[17] B. Nikoobakht, M.A. El-sayed, Chem. Mater. 15 (2003) 1957.

[18] T. Tohidi Moghadam, B. Ranjbar, K. Khajeh, Int. J. Biol. Macromol. 51 (2012) 91.

[19] A.D. McNaught, A. Wilkinson, IUPAC. Compendium of Chemical Terminology, in the "Gold Book, 2nd ed., Oxford: Blackwell Scientific Publications Oxford (United Kingdom), 1997, p. 1361.

[20] Z. Ma, L. Tian, T. Wang, C. Wang, Anal. Chim. Acta 673 (2010) 179.

[21] W. He, C.Z. Huang, Y.F. Li, J.P. Xie, R.G. Yang, P.F. Zhou, J. Wang, Anal. Chem. 80 (2008) 8424.

[22] H. Pei, F. Li, Y. Wan, M. Wei, H. Liu, Y. Su, N. Chen, Q. Huang, C. Fan, J. Am. Chem. Soc. 134 (2012) 11876.

[23] H.D. Hill, J.E. Millstone, M.J. Banholzer, C.A. Mirkin, ACS Nano 3 (2009) 418.

[24] G. Kawamura, Y. Yang, M. Nogami, J. Phys. Chem. C 112 (2008) 10632.

[25] J.G. Mehtala, D.Y. Zemlyanov, J.P. Max, N. Kadasala, S. Zhao, A. Wei, Langmuir 30 (2014) 13727.

[26] D. Yao, T. Song, B. Zheng, S. Xiao, F. Huang, H. Liang, Nanotechnology 26 (2015) 425601.

[27] I.C. Pekcevik, L.C.H. Poon, M.C.P. Wang, B.D. Gates, Anal. Chem. 85 (2013) 9960.

[28] J.P. Leal, J.M.S.S. Esperança, M.E. Minas da Piedade, J.N. Canongia Lopes, L.P.N. Rebelo, K.R. Seddon, J. Phys. Chem. A 111 (2007) 6176.

[29] Y. Jin, P. Wang, D. Yin, J. Liu, L. Qin, N. Yu, G. Xie, B. Li, Colloids Surfaces A Physicochem. Eng. Asp. 302 (2007) 366.

[30] T. Tohidi Moghadam, B. Ranjbar, Talanta, 144 (2015) 778.

[31] N.N. Brandt, A.Y. Chikishev, A.A. Mankova, I.K. Sakodynskaya, J. Biomed. Opt. 20 (2015) 1.